Journal of Colloid and Interface Science **256,** 378–395 (2002)
doi:10.1006/jcis.2002.8680

Evaluation of the Structural and Energetic Heterogeneity of Microporous Carbons by Means of Novel Numerical Methods and Genetic Algorithms

P. Kowalczyk,* A. P. Terzyk,†,[1] P. A. Gauden,† V. M. Gun'ko,‡ and L. Solarz§

*Military Institute of Chemistry and Radiometry, Department of Respiratory Protection, gen. Chruściel Avenue 105, 00-910 Warsaw, Poland; †N. Copernicus University, Department of Chemistry, Physicochemistry of Carbon Materials Research Group, Gagarin St. 7, 87-100 Toruń, Poland; ‡Institute of Surface Chemistry, 17 General Naumov Street, 03164 Kiev, Ukraine; and §Institute of Physics, Military Technical Academy, Kaliski St. 2, 00-908 Warsaw, Poland

Received May 21, 2002; accepted September 4, 2002

The main purpose of this study is to present a new method of evaluation of the heterogeneity of microporous carbons (called the LAPLACE method). The simple genetic algorithm (SGA) is modified and applied to the study of the LAPLACE method. The applicability of this procedure as well as the CONTIN package is checked based on new adsorption isotherm equations derived for two model pore size distributions (trapezoidal and bitriangular). The obtained results show that the proposed procedure and algorithm can be successfully used for the evaluation of the heterogeneity of microporous carbons. This procedure, as well as other (namely the Jaroniec–Choma equation, DFT theory, Nguyen–Do, and Horvath–Kawazoe) methods, together with the distributions of adsorption potential and adsorption energy, is applied to the characterization of series of commercially available carbons. © 2002 Elsevier Science (USA)

Key Words: **adsorption; active carbon; CONTIN; DA; DFT; HK; Nguyen-Do method.**

INTRODUCTION

A great many porous materials are characterized by structural and energetic heterogeneity (1–6). One of the most important problems of characterization of porous solids is the evaluation of the distribution of pores, especially of micropores (i.e., pores with a diameter smaller than 2 nm, according to the IUPAC classification (7, 8)) from the adsorption data. The theoretical description of physical and chemical adsorption on heterogeneous porous solids is based on the general adsorption integral equation (GAI) (1–5, 9–11). This concept leads to the use of the homotattic patch approximation, which assumes that the porous solids surface consists of an array of patches being geometrically and energetically uniform. The dimensions of such patches are small compared with the total adsorbing area, so when there is a large number of patches then the geometrical (e.g., pore radius and/or pore width) or energetical (e.g., adsorption energy) distribution can be considered to be continuous.

From the mathematical point of view, the assumptions mentioned above lead to a linear Fredholm integral equation of the first kind, which can be written in the following general form (12):

$$g(s) = \int_a^b K(t, s) f(t)\, ds. \qquad [1]$$

Here, $f(t)$ is an unknown function which should be found, while $g(s)$ is a known one. The function of two variables $K(t, s)$ is the kernel. Note that integral Fredholm equations, as opposed to integral Volterra equations, involve define integrals with fixed lower and upper limits (a and b in Eq. [1], respectively). Equation [1] is the analogue to the matrix equation

$$\mathbf{g} = \mathbf{K} \cdot \mathbf{f}, \qquad [2]$$

whose solution is $\mathbf{f} = \mathbf{K^{-1}} \cdot \mathbf{g}$, where $\mathbf{K^{-1}}$ is the inverse matrix. Like Eq. [1], Eq. [2] has a unique solution whenever $\mathbf{g}$ is nonzero (the homogenous case with $\mathbf{g} = \mathbf{0}$ is hardly ever useful) and $\mathbf{K}$ is invertible.

In the field of adsorption science the kernel $K(t, s)$ represents the adsorption model (e.g., the local adsorption isotherm on a homotactic patch of the solid surface), $g(s)$ denotes the experimental function (e.g., the overall adsorption isotherm), and $f(t)$ is the unknown pore or adsorption energy distribution.

Unfortunately, all the linear Fredholm integral equations of the first kind formulated on the ground of adsorption science are ill-posed (1–4, 9–11). That means that the right side of the presented equation is not known accurately, so we, in general, should formulate the problem as (13, 14)

$$g(s) + \varepsilon(s) = \int_a^b K(t, s) f(t)\, dt, \qquad [3]$$

where $\varepsilon(s)$ represents an error term and is an arbitrary function except for some condition with respect to the size of $\varepsilon(s)$, such as $|\varepsilon(s)| \le M$ or $\int_a^b \rho(s)\varepsilon^2(s)\, ds \le \bar{M}$, $\rho(s) > 0$ (where M and/or

[1] To whom correspondence should be addressed. E-mail: aterzyk@chem.uni.torun.pl.

0021-9797/02 $35.00
© 2002 Elsevier Science (USA)
All rights reserved.

$\bar{M}$ can be treated as the maximum experimental error (upper limit of error value) and/or as the maximum average experimental error) (14). Instead of a unique solution of Eq. [3] we get a family of solutions Ω. The real problem then is to pick out of the family of functions Ω the true solution Ψ. This cannot be done without more information about the problem stated in Eq. [3]. However, we can assume that the true solution Ψ is a reasonably smooth function. So the smoothness of the unknown distribution function $f(t)$ was used as an additional minimizing condition for the stabilization of the solution. Basing on such an assumption, the classical least square functional defined as (13)

$$\text{Minimize} \left\| g(s) - \int_a^b K(t,s) f(t)\, dt \right\|^2 \quad \text{with respect to } f(t) \qquad [4]$$

should be replaced by the functional (15)

$$\text{Minimize} \left\| g(s) - \int_a^b K(t,s) f(t)\, dt \right\|^2 + \Pi[f(t)] \quad \text{with respect to } f(t), \qquad [5]$$

where $\Pi[f(t)]$ is an additional term (i.e., penalty function (16)) for the stabilization of the solution. In the well-known regularization method, the term can be written in three alternative forms (13, 14, 17):

$$\Pi[f(t)] = \alpha \int_a^b f(t)^2\, dt \qquad [6a]$$

$$\Pi[f(t)] = \alpha \int_a^b \left[\frac{\partial^2 f(t)}{\partial t^2} \right]^2 dt \qquad [6b]$$

$$\Pi[f(t)] = \alpha \int_a^b \left[\frac{\partial^n f(t)}{\partial t^n} \right]^2 dt. \qquad [6c]$$

Here α is a regularization parameter and it is the mutual weighting of both terms in Eq. [5].

On the other hand, it is possible to incorporate a smoothing condition into Eq. [4] as follows (18):

$$\text{Minimize} \left\| g(s) - \int_a^b K(t,s) \cdot \sum_{i=1}^{N} w_i \xi_i(t)\, dt \right\|^2 \quad \text{with respect to } f(t). \qquad [7]$$

Here N is a number of trial functions $\xi_i(t)$ derived from a complete set forming a basis in a Hilbert space. Obviously, the number, position, and shape of the chosen functions strictly depend on the considered physical problem. The unknown coefficients w_i are now estimated by orthogonalizing the residual in Eq. [7] with respect to a suitably chosen set of functions.

In the current paper, two alternative approaches based on the theory of micropore filling (TOMF) are presented and used to evaluate the micropore size distributions (MPSD) from both generated (pure and disturbed by Gaussian error (19)) and some experimental adsorption isotherms. First, the well-known CONTIN algorithm written by Provencher (20, 21) was modified and used to solve the adsorption integral equation with Dubinin–Radushkevich (DR) (7) or Dubinin–Astakhov (DA) (7) equations as a kernel. Although both equations are thermodynamically inconsistent (4, 9, 22, 23), they still remain the most frequently used for the characterization of microporosity of activated carbons. Moreover, as was shown recently by Condon (24, 25), both equations may be derived from an isotherm equation that has its basis in simple quantum-mechanical assumptions.

Second, a new LAPLACE algorithm based on both Laplace transforms and optimization by evolutionary algorithms was developed and adopted to determine the structural heterogeneity of microporous activated carbons on the basis of the TOMF. A simple strategy for stabilizing an ill-posed problem is to reduce the number of degrees of freedom by fitting a parameterized solution to the data. The well-known Jaroniec–Choma equation with gamma distribution is an example of this method. This model, originally proposed by Jaroniec and co-workers (26), was used to determine the MPSD from the experimental data. The results obtained on the basis of the TOMF are compared with those obtained from density functional theory (DFT) (27–31) from the Nguyen and Do method (ND) (32–35) and from the Horvath and Kawazoe procedure (HK) (36–42). Moreover, the adsorption potential (APD) (43) and adsorption energy (AED) (1, 2, 4, 11, 35, 44–46) distributions are evaluated from experimental low-temperature nitrogen adsorption isotherms.

NOVEL METHOD AND NUMERICAL ALGORITHM APPLIED TO THE EVALUATION OF THE MPSD FUNCTION

In the current study, for the description of adsorption on structurally heterogeneous microporous solids, the following form of the linear Fredholm integral equations of the first kind (i.e., with DR and/or DA equations as a kernel) is assumed (1–5, 9–11, 40, 47, 48),

$$\Theta_{\text{global}}(p) = \int_{B_{\min}}^{B_{\max}} \exp\left[-B \left(\frac{A}{\beta} \right)^n \right] f(B)\, dB, \qquad [8]$$

where $\Theta_{\text{global}}(p)$ is the experimental (overall) adsorption isotherm, $A = -\Delta G = RT \ln(p_0/p)$ is the adsorption potential, defined as change in the Gibbs free energy taken with a minus sign, B is a structural parameter equal to $(1/E_0)^n$, R is the universal gas constant, T is temperature, p and p_0 denote the equilibrium pressure and the saturation vapor pressure,

respectively, β is the similarity coefficient, equal to 0.292, for nitrogen (49), and n is the equation parameter, equal to 2 for the DR isotherm. A number of relations between the parameter of micropore structure (micropore half-width) and B have been developed up till now (see references in (50)). The best known of them, originally proposed by Dubinin (51), is defined by

$$x^n = \frac{C^n}{B}. \quad [9]$$

For the adsorption of nitrogen on activated carbons Bhatia and Shethna (49) assumed $C = 11.4$. Knowing the $f(B)$, the micropore size distribution (MPSD) can be obtained using the following transformations:

$$f(x) = f(B)\frac{dB}{dx} \quad [10]$$

$$f(x) = -Cx^{-n-1}f(B) \quad [11]$$

Developed by Provencher (20, 21), CONTIN is a package for solving noisy linear integral equations of the first kind and system of (possibly ill-conditioned) linear algebraic equations. This program suit is often applied to solve integral equations of the first kind with respect to effectively continuous distributions of diffusion coefficients, molecular weights, relaxation times, electron densities, adsorption energy distributions (46, 52–58), pore size distributions (35, 52, 55–60), etc. As mentioned above, in CONTIN the regularization method was used for the stabilization of solution. In CONTIN the classical functional of the form

$$\text{Minimize} \sum_{i=1}^{L_C} \left\| \Theta_i - \int_{B_{\min}}^{B_{\max}} \exp[-By_i]\, f(B)\, dB \right\|^2 \quad \text{with respect to } f(B), \quad [12]$$

where L_C is a number of isotherm points, is replaced by the functional proposed by Provencher (61);

$$\text{Minimize} \sum_{i=1}^{L_C} \left\| \Theta_i - \int_{B_{\min}}^{B_{\max}} \exp[-By_i]\, f(B)\, dB \right\|^2 + \alpha \| f''(B)^2 \| \quad \text{with respect to } f(B), \quad [13]$$

where $f''(B)$ is the second derivative of $f(B)$ (it is unknown (estimated) distribution of B and α is a regularization parameter determined in CONTIN using a Bayesian approach. We want to point out here that there are no assumptions as to shape and the sign of $f(B)$ in CONTIN package; however, applying natural condition of no negativity of $f(B)$ at any B one can obtain stable solution possessing physical meaning.

Following Dubinin and Stoeckli (47), the approximate solution of Eq. [8] can be obtained over the integration range $(0, \infty)$. The most familiar reason for using such an integration range is related to the simplification of the problem defined by Eq. [8] (one should notice that limitation or no limitation of the integration range does not practically affect the shape of the distribution functions with respect to the pore size or adsorption energy). The above assumption leads to a Laplace transform (12) defined as

$$\aleph\{f\} = \Theta_{\text{global}}(p) = \int_0^\infty \exp[-By] f(B)\, dB, \quad [14]$$

implying that $y = (A/\beta)^n$. Both $\Theta_{\text{global}}(p)$ and $f(B)$ were approximated on $(0, \infty)$ by

$$\Theta_{\text{global}}(p) \cong \sum_{j=1}^{M_f} w_j \eta_j(p) \quad [15]$$

$$f(B) \cong \sum_{j=1}^{M_f} w_j \varphi_j(B, B_{0j}), \quad [16]$$

where M_f is a number of base functions, w_j is a vector of weights, $\varphi_j(B, B_{0j})$ is a series of base functions defined below (Eq. [18]), $\eta_j(p)$ is a series of functions approximating the global adsorption isotherms $\theta_{\text{global}}(p)$, and B_{0j} is an average value of the jth base function.

As a result of these transformations, an approximate formula for $\Theta_{\text{global}}(p)$ can be expressed by

$$\Theta_{\text{global}}(p) = \int_0^\infty \exp[-By] \sum_{j=1}^{M_f} w_j \varphi_j(B, B_{0j})\, dB. \quad [17]$$

The functions $\varphi_j(B, B_{0j})$ can be represented by the form (some base functions used for approximation bimodal microporous structure of activated carbons are presented in Fig. 1)

$$\varphi_j(B, B_{0j}) = \frac{B}{B_{0j}} \exp\left[-\omega \left| \frac{B}{B_{0j}} - 1 \right| \right], \quad [18]$$

where ω is a parameter which forms base functions across modification of its standard deviation. Note that the base functions defined above are very similar shape to real functions consisting of several peaks.

The solution of Eq. [17] possesses the form

$$\Theta_{\text{global}}(p) = \sum_{j=1}^{M_f} w_j (B_{0j}\{\exp[-\omega]\Omega_j(B, B_{0j}) + \exp[\omega]\Psi_j(B, B_{0j})\}), \quad [19]$$

where

$$\Omega_j(B, B_{0j}) = \frac{1}{(\omega - B_{0j}y)} \left\{ \frac{1}{(\omega - B_{0j}y)} + \exp[\omega - B_{0j}y] \times \left[1 - \frac{1}{(\omega - B_{0j}y)} \right] \right\} \quad [20]$$

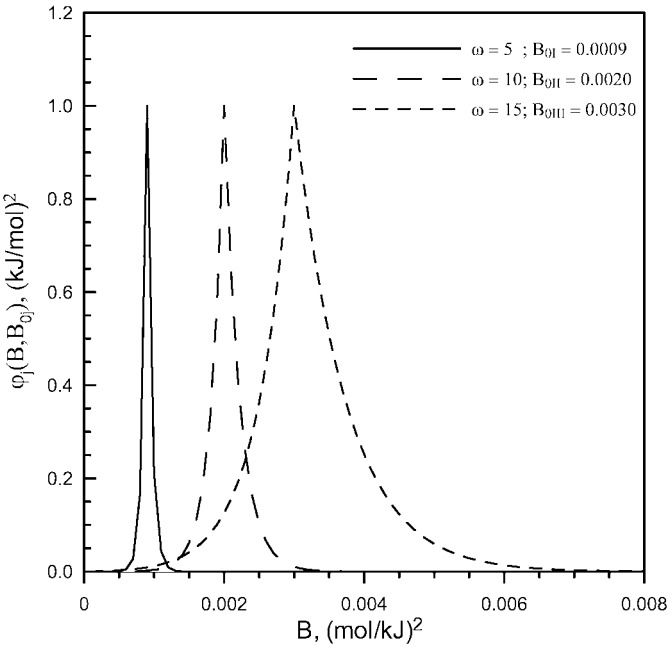

FIG. 1. Some base functions $\varphi_j(B, B_{0j})$ used for approximation of bi microporous structure of activated carbons.

$$\Psi_j(B, B_{0j}) = \frac{1}{(\omega + B_{0j}y)}\left\{\exp[-B_{0j}y - \omega] \times \left[1 + \frac{1}{(\omega + B_{0j}y)}\right]\right\}. \quad [21]$$

One can see that the problem of solving Eq. [8] (i.e., the adsorption integral equation) was transformed, in the approach proposed in this study, into the minimization of the following functional:

$$\text{Minimize}\prod = \int_{p_{\min}}^{p_{\max}} \left\| \Theta_{\text{global}}(p) - \sum_{j=1}^{M_f} w_j \Delta_j(B, B_{0j}) \right\| dp \quad [22]$$

with respect to w_j, B_{0j} ($j = 1, 2, \ldots, M_f$), and

$$\Delta_j(B, B_{0j}) = B_{0j}\{\exp[-\omega]\Omega_j(B, B_{0j}) + \exp[\omega]\Psi_j(B, B_{0j})\}. \quad [23]$$

As clearly shown in a series of earlier papers, the micropores usually tend to group into two patches. Following this observation, Eq. [21] can be reduced to a biporous structure of micropore size distribution,

$$\text{Minimize}\prod = \int_{p_{\min}}^{p_{\max}} \| \Theta_{\text{global}}(p) - w_1\Delta_1(B, B_{01}) - w_2\Delta_2(B, B_{02}) \| dp, \quad [24]$$

with respect to w_1, B_{01}, w_2, and B_{02}.

In the current search for optimal parameters (i.e., w_1, B_{01}, w_2, and B_{02}), a modification of the simple genetic algorithm (SGA) with real coding was developed. Such a novel optimization technique, proposed by Holland (62) and developed by Goldberg (63), belongs to "special artificial intelligence techniques." The SGA maintains a population of individuals, $P(t) = \{x_1^t, \ldots, x_n^t\}$, for iteration t (19). Each individual represents a potential solution to the problem at hand and is implemented as some data structure (i.e., structure, object, and so on). Each solution x_i^t is evaluated to give some measure of its "fitness." Then a new population (iteration $t + 1$) is formed by selecting more fitting individuals (selection step by means of modified roulette wheel). Some members of the new population undergo transformation by means of "genetic" operators (simple crossover and classical mutation) to form new solutions. After some number of generations (stop condition) the algorithm converges. The best individual is hoped to represent a near-optimum (reasonable) solution.

OTHER METHODS OF THE EVALUATION OF MPSD

Different alternative methods of solution of Eq. [8] have been proposed based on the theory of micropore filling (TOMF) (1–5, 10, 26, 40, 47, 64–70). For example, Jaroniec and Choma suggested one of them (26). They approximated the unknown distribution function $f(B)$ by a monomodal gamma-type distribution. Additionally, the authors assumed that a micropore region (i.e., integration boundaries) $x \in (0, \infty)$ could be accepted. Taking those assumptions into account Jaroniec and co-workers parameterized the integral equation defined by Eq. [8] and obtained a simple formula for the overall adsorption isotherm ($\Theta_{\text{global}}(p)$) in micropores:

$$\Theta_{\text{JCh}}(p) = \left[1 + \left(\frac{A}{\beta\rho}\right)^n\right]^{-\frac{v}{n}}. \quad [25]$$

The MPSD (assuming a model of slit-like micropores) can be obtained applying simple transformations,

$$F(z) = \frac{n\rho^v}{\Gamma(v/n)} z^{v-1} \exp[-(\rho z)^n], \quad [25a]$$

where $z = E_0^{-1}$, $x = Cz$, $f(x) = F(z)(dx/dz)^{-1}$, and $B = z^n$.

Due to the simplicity of Eq. [25], this isotherm has been used to fit many experimental data to obtain such structural parameters as n, ρ, and v. This method should be used with some caution because if the true MPSD does not confirm to the assumed form, the derived MPSD can be erroneous (40, 60).

As has recently been reported, molecular models of adsorption such as density functional theory (DFT) (27–31) and Monte Carlo (MC) (30, 31, 71–73) simulations can be successfully applied to the description of adsorption phenomena. Based on given intermolecular potentials of fluid–fluid and fluid–solid interaction, they allow the construction of adsorption isotherms in model pores. With a set of model isotherms in individual pores,

the experimental isotherm can be described as a superposition of the model isotherms and the pore size distribution. Such assumptions lead to the linear Fredholm integral equation of the first kind (74)

$$\Theta_{\text{global}}(p) = \int_{L_{\min}}^{L_{\max}} \Theta_{\text{local}}(p, L)\,\varphi(L)\,dL, \qquad [26]$$

where $\Theta_{\text{local}}(p, L)$ is a theoretical isotherm in a model pore of size $L(\equiv 2x$, where x is the half–width of a pore), and $\varphi(L)$ is the pore size distribution. The pore size distributions (PSD and MPSD) were calculated using the DFT software from Micromeritics (NORCROSS, GA) (74). A local mean field DFT was first used by Seaton and co-workers (28). Olivier and coworkers (27, 29) improved this method using a nonlocal mean field DFT.

Nguyen and Do (32–35) developed a new method for the evaluation of pore size distributions from adsorption data. The procedure is based on the combination of the Kelvin equation and the statistical adsorbed film thickness. The most important feature of this method is the possibility of analysis of the structural heterogeneity of porous solids without separate approaches to micro and mesopores. Additionally, it provides results close to those obtained using the DFT method mentioned above (34, 35). Following Nguyen and Do's method the local adsorption isotherm equation possesses the form (32–35)

$$a = \int_{r_{\min}}^{r_k(p)} f(R_p)\,dR_p + \int_{r_k(p)}^{r_{\max}} \frac{w_{\text{NG}}}{R_p} t(p, R_p) f(R_p)\,dR_p, \qquad [27]$$

where $r_{\min}$ and $r_{\max}$ are the minimal and maximal half-widths (or pore radii), respectively; $W_{\text{NG}} = 1$ for slit like pores and 2 for cylindrical pores; $r_k(p)$ is determined with the Kelvin equation (γ is the liquid surface tension; ν_{m} is the liquid molar volume; θ is the liquid–solid contact angle)

$$r_k(p) = \frac{\sigma_{\text{s}}}{2} + t(p, R_p) + \frac{w_{\text{NG}}\gamma\nu_{\text{m}}\cos(\theta)}{RT\ln(p_0/p)}, \qquad [28]$$

where the statistical adsorbed film thickness is equal to

$$t(p, R_p) = t_m \frac{c_{\text{B}} z_{\text{B}}}{(1 - z_{\text{B}})} \times \left[\frac{1 + (n_{\text{B}}b/2 - n_{\text{B}}/2)z_{\text{B}}^{n-1} - (n_{\text{B}}b + 1)z_{\text{B}}^{n} + (n_{\text{B}}b/2 + n_{\text{B}}/2)z_{\text{B}}^{n+1}}{1 + (c_{\text{B}} - 1)z_{\text{B}} + (c_{\text{B}}b/2 - b/2)z_{\text{B}}^{n} - (c_{\text{B}}b/2 + b/2)z_{\text{B}}^{n+1}}\right], \qquad [29]$$

$t_m = a_m/S_{\text{BET}}$ (thickness of a single layer of the adsorbate); a_m is the BET monolayer capacity; S_{BET} is the BET specific surface area; $t(p, R_p)$ is the statistical thickness of adsorbed layer; $b = \exp(\Delta\varepsilon/RT)$; $\Delta\varepsilon$ is the excess of the evaporation heat due to the interference of the layering on the opposite wall of pores (typically $\Delta\varepsilon$ is less than 3 kJ mol^{-1}; in (32, 33) $\Delta\varepsilon \approx 2.2$ kJ mol^{-1}); $c_{\text{B}} = c_{s,\text{B}} \exp\lfloor(Q_p - Q_s)/RT\rfloor$; $c_{s,\text{B}}$ is the BET coefficient for adsorption on a "flat" surface; Q_s and Q_p are the adsorption heat on flat surface and in pores, respectively; $z_{\text{B}} = p/p_0$; n_{B} is the number (noninteger) of statistical monolayers of adsorbate molecules and its maximal value for the given R_p (or pore half-width x) is equal to $(R_p - \sigma_s/2)/t_m$; and σ_s is the collision diameter of surface atoms ($\sigma_s = 0.34$ nm for C atoms on carbon surfaces). Adsorption data were used to compute the $f(x)$ distribution with Eq. [27] and regularization procedure under nonnegativity condition with unfixed one (automatically determined on the basis of F-test and confidence regions using the parsimony principle) within the scope of the slit-like pore model. Similar procedures with the direct minimization, local, and integral isotherm approximations were used previously to investigate the pore structure of different adsorbents [35].

Horvath and Kawazoe (HK) (36–42) proposed a simple method for evaluating the MPSD from a single gas adsorption isotherm. It is based on the thermodynamics of adsorption and for strictly microporous solids it leads for some cases to almost identical results as obtained from DFT method (10, 50, 75). In the case of the adsorption of nitrogen molecules on the activated carbon the HK equation is given by

$$\Psi(2d_p) = \ln\left(\frac{p}{p_0}\right) - \frac{62.38}{2d_p - 0.64} \times \left[\frac{1.895 \times 10^{-3}}{(2d_p - 0.32)^3} - \frac{2.7087 \times 10^{-7}}{(2d_p - 0.32)^9} - 0.05014\right] = 0. \qquad [30]$$

The MPSD can be directly obtained from the adsorption data by applying the transforms

$$\Psi(2d_p) = f\left(\frac{p}{p_0}\right) \qquad [31]$$

$$W_{\text{micropore}} = f\left(\frac{p}{p_0}\right) \qquad [32]$$

$$\frac{d}{d(2d_p)} W_{\text{micropore}} = \frac{d}{d(2d_p)} \Psi(2d_p), \qquad [33]$$

where d_p is the micropore half-width.

ENERGETIC HETEROGENEITY OF SOLIDS

Energetic heterogeneity of porous solids results from the structural heterogeneity (1–6, 10, 11, 53–60) (i.e., dispersion of pore sizes, surface irregularities such as defects in crystalline structure) and from the heterogeneity caused by differences in the energy of interactions of an adsorbate molecule with surface (the presence of different atoms and functional groups on carbon surface, mineral pollutions in carbon materials and so on). For the estimation of global energetic heterogeneity of porous solids several methods have been proposed up to the present.

The adsorption potential distribution is a simple method frequently used in the literature (43). APD may be easily obtained by numerical differentiation of the adsorption characteristic curve:

$$F(A) = -\frac{d\Theta(p)}{d[RT\ln(p_0/p)]} = -\frac{d\Theta(p)}{dA}. \quad [34]$$

Thus this is another method of presentation the adsorption isotherm. In spite of the simplicity of this procedure, the APD peak positions give information about distribution of energetic sites in the pore region. In the current studies the well-known interpolation by cubic spline is used for evaluation of the APDs from the measured nitrogen adsorption isotherms.

According to another theory, the distributions of adsorption energetic sites can be obtained by applying the linear Fredholm integral equation of the first kind (see Eqs. [1] and [26])

$$\Theta_{\text{global}}(p) = \int_{E_{\min}}^{E_{\max}} \Theta_{\text{local}}(p, E) f(E)\, dE, \quad [35]$$

where $\Theta_{\text{local}}(p, E)$is a local adsorption isotherm describing an adsorption process on energetically homogenous surface, and $f(E)$ is the distribution of adsorption energy. The Fowler–Guggenheim equation (describing localized monolayer adsorption with lateral interaction) was frequently used as a kernel of Eq. [35] (1, 2, 4–6, 11, 35, 53–58),

$$\Theta_{\text{local}}(p, E) = \frac{K_{\text{FG}} p \exp[z_{\text{FG}} w_{\text{FG}} \Theta_{\text{FG}}/k_{\text{B}}T]}{1 + K_{\text{FG}} p \exp[z_{\text{FG}} w_{\text{FG}} \Theta_{\text{FG}}/k_{\text{B}}T]}, \quad [36]$$

where $K_{\text{FG}} = K_{0\text{FG}}(T)\exp[E/k_{\text{B}}T]$ is the Langmuir constant for adsorption on monoenergetic sites and the preexponential factor $K_{0\text{FG}}(T)$ is expressed in terms of the partition functions for an isolated gas and surface phases, z_{FG} is a number of nearest neighbors of an adsorbate molecule (assuming $z_{\text{FG}} = 4$), w_{FG} is the interaction energy between a pair of nearest neighbors, k_{B} is the Boltzman constant ($z_{\text{FG}} w_{\text{FG}}/k_{\text{B}} = 380$ K). For the evaluation of $f(E)$ from measured nitrogen adsorption isotherms a modification of the CONTIN package was applied (53–58).

To describe all distributions obtained in this paper several magnitudes such as surface area under the distribution, mean, variance, dispersion, and skew were used. The values of these parameters are determined on the ground of equalizations based on the theory of statistical moments (76),

$$\Omega = \int_{\zeta_{\min}}^{\zeta_{\max}} \left(\frac{\partial\Theta(p)}{\partial\zeta}\right) d\zeta \quad [37]$$

$$\bar{\zeta} = \frac{\int_{\zeta_{\min}}^{\zeta_{\max}} \zeta\left(\frac{\partial\Theta(p)}{\partial\zeta}\right) d\zeta}{\Omega} \quad [38]$$

$$\delta = \frac{\int_{\zeta_{\min}}^{\zeta_{\max}} (\zeta - \bar{\zeta})^2\left(\frac{\partial\Theta(p)}{\partial\zeta}\right) d\zeta}{\Omega} \quad [39]$$

$$\sigma = \sqrt{\delta} \quad [40]$$

$$\chi = \frac{\int_{\zeta_{\min}}^{\zeta_{\max}} (\zeta - \bar{\zeta})^3\left(\frac{\partial\Theta(p)}{\partial\zeta}\right) d\zeta}{\Omega}, \quad [41]$$

where ζ denotes the micropore half-width (or adsorption energy) and $\zeta_{\min}$ and $\zeta_{\max}$ are the upper and lower limits of the analyzed distribution, respectively; Ω is the surface urea under the pore (adsorption energy) distribution; $\bar{\zeta}$ is the mean, δ is the variance, σ is the standard deviation, and χ is the skew. The characteristics were calculated for the ranges of the pore half-widths and energies where strongly marked peaks occur.

THE NEW ISOTHERM EQUATIONS FOR ADSORPTION ON HETEROGENEOUS MICROPOROUS SOLIDS

As mentioned by Rudziński and Everett (1), really existing heterogeneous solids can be characterized by a complicated form of MPSD, with a number of local minima and maxima. However, with a certain degree of accuracy, the real MPSD curve can be (for practical purposes) approximated by some "smoothed" functions and their shape is described by a small number of parameters. Certainly, when the proposed model of the MPSD does not describe the equilibrium data well a series of "smoothed" functions should be introduced.

New adsorption isotherm equations developed in this section (assuming a trapezoidal or bitriangular form of distribution function $f(B)$; ζ_i and m are the parameters determining the shape and height of $f(B)$, respectively; notations are given in Fig. 2) were chosen in the investigations on the stability of the proposed algorithms (CONTIN and LAPLACE) used for the evaluation of MPSD from the adsorption data. The numerical investigations were performed by applying both pure generated and disturbed with Gaussian noise (19, 77, 78) nitrogen adsorption isotherms. Analytical forms of the overall adsorption isotherms (assuming the DA equation as a kernel) are presented below.

The Trapezoidal Representation of $f(B)$

$$f(B) = \begin{cases} \dfrac{\Phi(\zeta_b)}{\zeta_b - \zeta_a}(B - \zeta_a) & \zeta_a \le B < \zeta_b \\ \Phi(\zeta_b) & \zeta_b \le B < \zeta_c \\ \dfrac{\Phi(\zeta_b)}{\zeta_c - \zeta_d}(B - \zeta_d) & \zeta_c \le B \le \zeta_d \\ 0 & \text{elsewhere.} \end{cases} \quad [42]$$

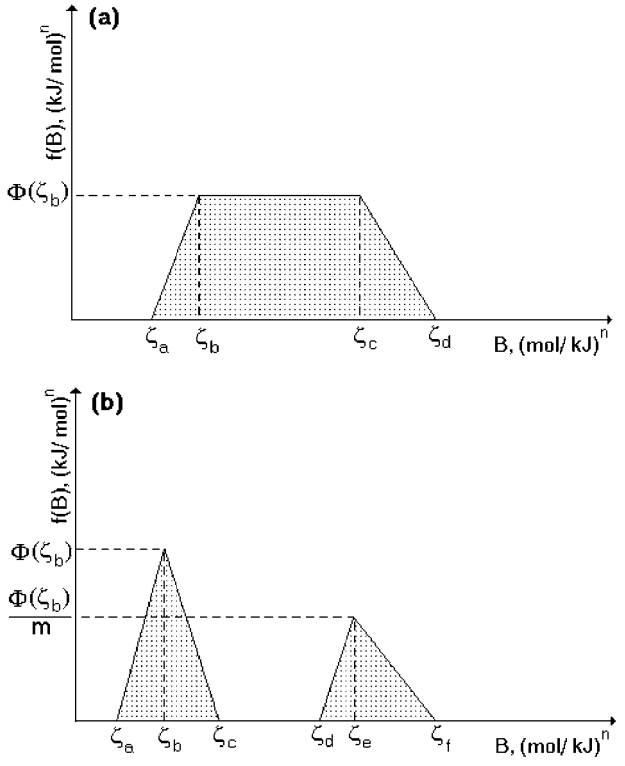

FIG. 2. The shapes of model functions: (a) (---) trapezoidal and (b) (—) bi-triangle used for the representation of the $f(B)$ distribution.

Normalization factor:

$$\Phi(\zeta_b) = \frac{2}{(\zeta_d - \zeta_a) + (\zeta_c - \zeta_b)}. \quad [43]$$

Isotherm equation:

$$\Theta(p) = K_1(p) + K_2(p) + K_3(p) + K_4(p) + K_5(p), \quad [44]$$

where

$$K_1(p) = -\frac{\Phi(\zeta_b)}{(\zeta_b - \zeta_a)}\zeta_a y^{-1}\{\exp[-\zeta_a y] - \exp[-\zeta_b y]\} \quad [45]$$

$$K_2(p) = \frac{\Phi(\zeta_b)}{(\zeta_c - \zeta_d)} y^{-1}\{(\zeta_c + y^{-1})\exp[-\zeta_c y] - (\zeta_d + y^{-1}) \times \exp[-\zeta_d y]\} \quad [46]$$

$$K_3(p) = \Phi(\zeta_b)\, y^{-1}\{\exp[-\zeta_b y] - \exp[-\zeta_c y]\} \quad [47]$$

$$K_4(p) = -\frac{\Phi(\zeta_b)}{(\zeta_c - \zeta_d)}\zeta_d y^{-1}\{\exp[-\zeta_c y] - \exp[-\zeta_d y]\} \quad [48]$$

$$K_5(p) = \frac{\Phi(\zeta_b)}{(\zeta_b - \zeta_a)} y^{-1}\{(\zeta_a + y^{-1})\exp[-\zeta_a y] - (\zeta_b + y^{-1})\exp[-\zeta_b y]\}. \quad [49]$$

The Bitriangular Representation of $f(B)$

$$f(B) = \begin{cases} \dfrac{\Phi(\zeta_b)}{\zeta_b - \zeta_a}(B - \zeta_a) & \zeta_a \le B < \zeta_b \\ \dfrac{\Phi(\zeta_b)}{\zeta_b - \zeta_c}(B - \zeta_c) & \zeta_b \le B < \zeta_c \\ \dfrac{\Phi(\zeta_b)}{m(\zeta_e - \zeta_d)}(B - \zeta_d) & \zeta_d \le B < \zeta_e \\ \dfrac{\Phi(\zeta_b)}{m(\zeta_e - \zeta_f)}(B - \zeta_f) & \zeta_e \le B < \zeta_f \\ 0 & \text{elsewhere.} \end{cases} \quad [50]$$

Normalization factor:

$$\Phi(\zeta_b) = \frac{1}{0.5 \cdot [(\zeta_c - \zeta_a) + m^{-1}(\zeta_f - \zeta_d)]}. \quad [51]$$

Isotherm equation:

$$\Theta(p) = K_6(p) + K_7(p) + K_8(p) + K_9(p) + K_{10}(p) + K_{11}(p) + K_{12}(p) + K_{13}(p), \quad [52]$$

where

$$K_6(p) = \frac{\Phi(\zeta_b)}{(\zeta_b - \zeta_a)} y^{-1}\{(\zeta_a + y^{-1})\exp[-\zeta_a y] - (\zeta_b + y^{-1})\exp[-\zeta_b y]\} \quad [53]$$

$$K_7(p) = -\frac{\Phi(\zeta_b)}{(\zeta_b - \zeta_a)}\zeta_a y^{-1}\{\exp[-\zeta_a y] - \exp[-\zeta_b y]\} \quad [54]$$

$$K_8(p) = \frac{\Phi(\zeta_b)}{(\zeta_b - \zeta_c)} y^{-1}\{(\zeta_b + y^{-1})\exp[-\zeta_b y] - (\zeta_c + y^{-1})\exp[-\zeta_c y]\} \quad [55]$$

$$K_9(p) = -\frac{\Phi(\zeta_b)}{(\zeta_b - \zeta_c)}\zeta_c y^{-1}(\exp[-\zeta_b y] - \exp[-\zeta_c y]) \quad [56]$$

$$K_{10}(p) = \frac{\Phi(\zeta_b)}{m(\zeta_e - \zeta_d)} y^{-1}\{(\zeta_d + y^{-1})\exp[-\zeta_d y] - (\zeta_e + y^{-1})\exp[-\zeta_e y]\} \quad [57]$$

$$K_{11}(p) = -\frac{\Phi(\zeta_b)}{m(\zeta_e - \zeta_d)}\zeta_d y^{-1}\{\exp[-\zeta_d y] - \exp[-\zeta_e y]\} \quad [58]$$

$$K_{12}(p) = \frac{\Phi(\zeta_b)}{m(\zeta_e - \zeta_f)} y^{-1}\{(\zeta_e + y^{-1})\exp[-\zeta_e y] - (\zeta_f + y^{-1})\exp[-\zeta_f y]\} \quad [59]$$

$$K_{13}(p) = -\frac{\Phi(\zeta_b)}{m(\zeta_e - \zeta_f)}\zeta_f y^{-1}\{\exp[-\zeta_e y] - \exp[-\zeta_f y]\}. \quad [60]$$

EXPERIMENTAL

Three commercial granulated activated carbons, D43/1 (Carbo-Tech, Essen, Germany), WD-extra, and AHD (Hajnówka, Poland), extensively investigated elsewhere (79–87), are the subject of this study. They were deashed using the two-step acid treatment method proposed by Korver. The detailed analysis of the procedure of deashing, as well as the mechanism of this process, was studied previously (79). Suspensions of the initial Polish carbons were strongly alkaline. This is why before the application of acids, the carbons were washed off with distilled water to obtain a neutral pH. After each step of Korver's method two carbon samples were obtained: one was treated with concentrated HCl (D43/1 treated, WD treated and AHD treated samples) and one was treated using both concentrated HCl and HF (D43/1 pure, WD pure, AHD pure). Finally, the carbons were washed using distilled water so that the conductivity of the suspension reached a value close to that of distilled water. Nitrogen adsorption isotherms were measured using a Micromeritics ASAP 2010 analyzer.

RESULTS AND DISCUSSION

First, the stability of both CONTIN and LAPLACE algorithms was investigated using generated (pure and disturbed with Gaussian errors) isotherms of adsorption in micropores. Four nitrogen isotherms were generated based on Eqs. [44] and [52] (see Fig. 3 caption for details) and then they were disturbed with Gaussian errors by the Box and Muller method

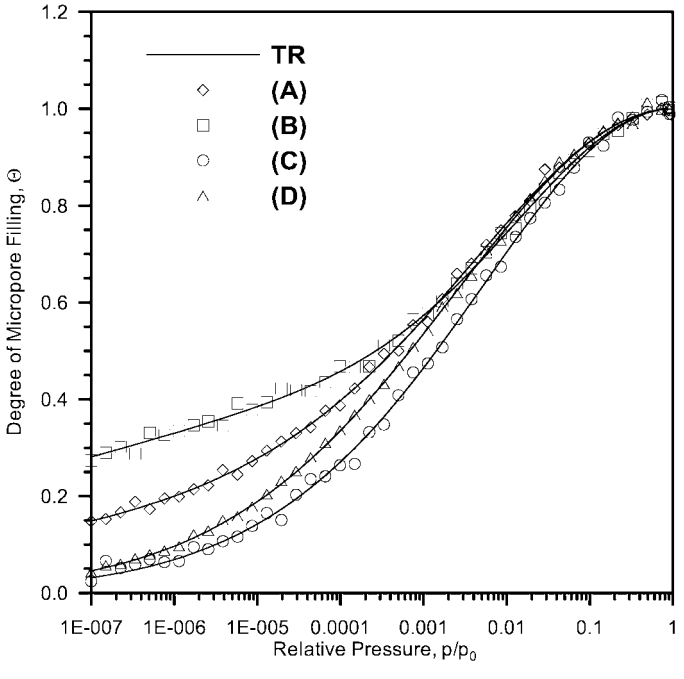

FIG. 3. Generated initial (TR) and disturbed with Gaussian error (points) nitrogen adsorption isotherms. The theoretical isotherms were obtained on the values of parameters: (A) $\varsigma_a = 0.0001$, $\varsigma_b = 0.0009$, $\varsigma_c = 0.001$, $\varsigma_d = 0.002$, $\varsigma_e = 0.003$, $\varsigma_f = 0.006$, $m = 0.5$ (Eq. [52]). (B) $\varsigma_a = 0.0002$, $\varsigma_b = 0.0003$, $\varsigma_c = 0.001$, $\varsigma_d = 0.0055$, $\varsigma_e = 0.0063$, $\varsigma_f = 0.007$, $m = 0.5$ (Eq. [52]). (C) $\varsigma_a = 0.001$, $\varsigma_b = 0.003$, $\varsigma_c = 0.005$, $\varsigma_d = 0.0055$, $\varsigma_e = 0.006$, $\varsigma_f = 0.007$, $m = 0.5$ (Eq. [52]). (D) $\varsigma_a = 0.001$, $\varsigma_b = 0.0025$, $\varsigma_c = 0.003$, $\varsigma_d = 0.0045$ (Eq. [44]).

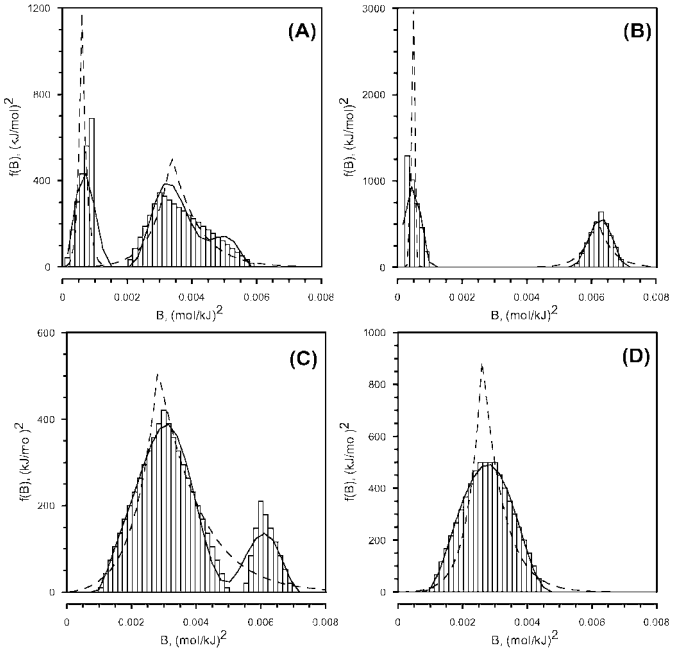

FIG. 4. The recovering results of pure nitrogen adsorption isotherms drawn in Fig. 3 as lines (bar theoretical $f(B)$, solid line (—) CONTIN algorithm, and dashed line (---) LAPLACE algorithm ($\omega = 3$)).

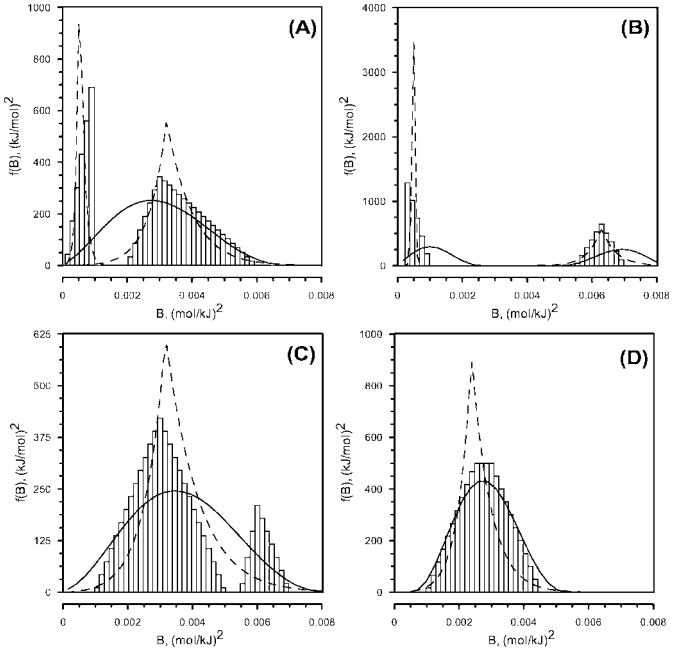

FIG. 5. The recovering results of disturbed with Gaussian error nitrogen adsorption isotherms drawn in Fig. 3 as points (bar theoretical $f(B)$, solid line (—) CONTIN algorithm, and dashed line (---) LAPLACE algorithm ($\omega = 3$)).

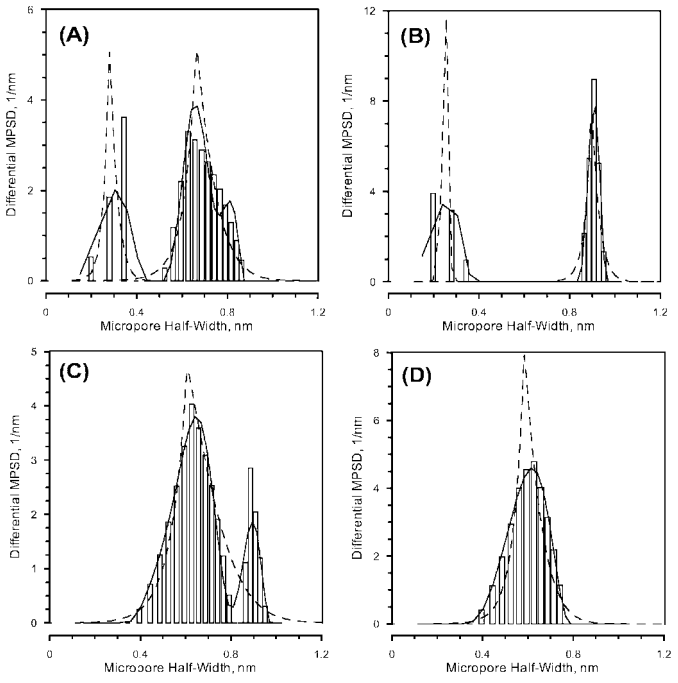

FIG. 6. The recovering results of pure nitrogen adsorption isotherms generated basing on the results presented in Fig. 4 (Eq. [11]) (bar theoretical MPSD, solid line (—) CONTIN algorithm, and dashed line (---) LAPLACE algorithm ($\omega = 3$)).

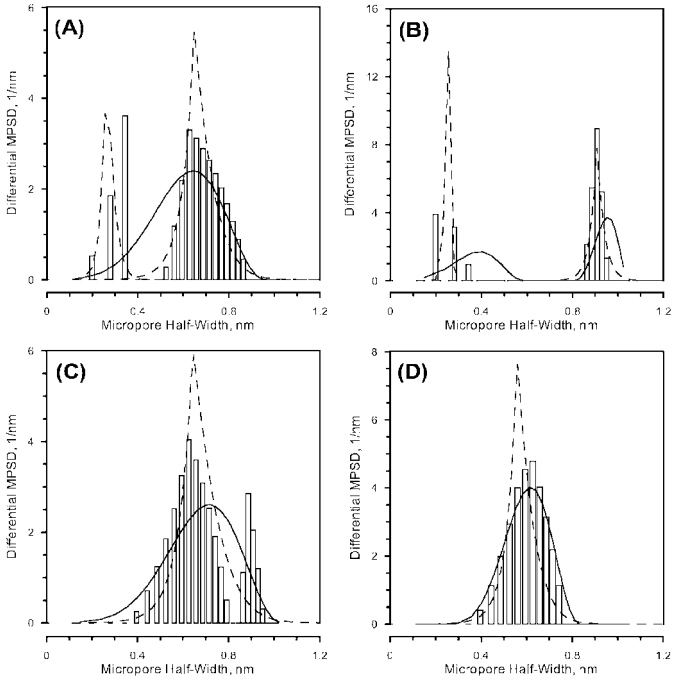

FIG. 7. The recovering results of disturbed with Gaussian error nitrogen adsorption isotherms generated basing on the results presented in Fig. 5 (Eq. [11]) (bar theoretical MPSD, solid line (—) CONTIN algorithm, and dashed line (---) LAPLACE algorithm ($\omega = 3$)).

(19, 77, 78). Obviously, due to the thermodynamic inconsistency of Dubinin's theory (9, 22, 23) the generated isotherms do not obey the Henry's law limit. As shown in Fig. 3, they differ significantly one from the other, especially in the low-pressure range. From Figs. 4–6 it arises that both the CONTIN and LAPLACE algorithms recover mono- and bimodal $f(B)$, as well as MPSD curves, reasonably well. The LAPLACE algorithm reproduces peaks that are narrower and higher than real

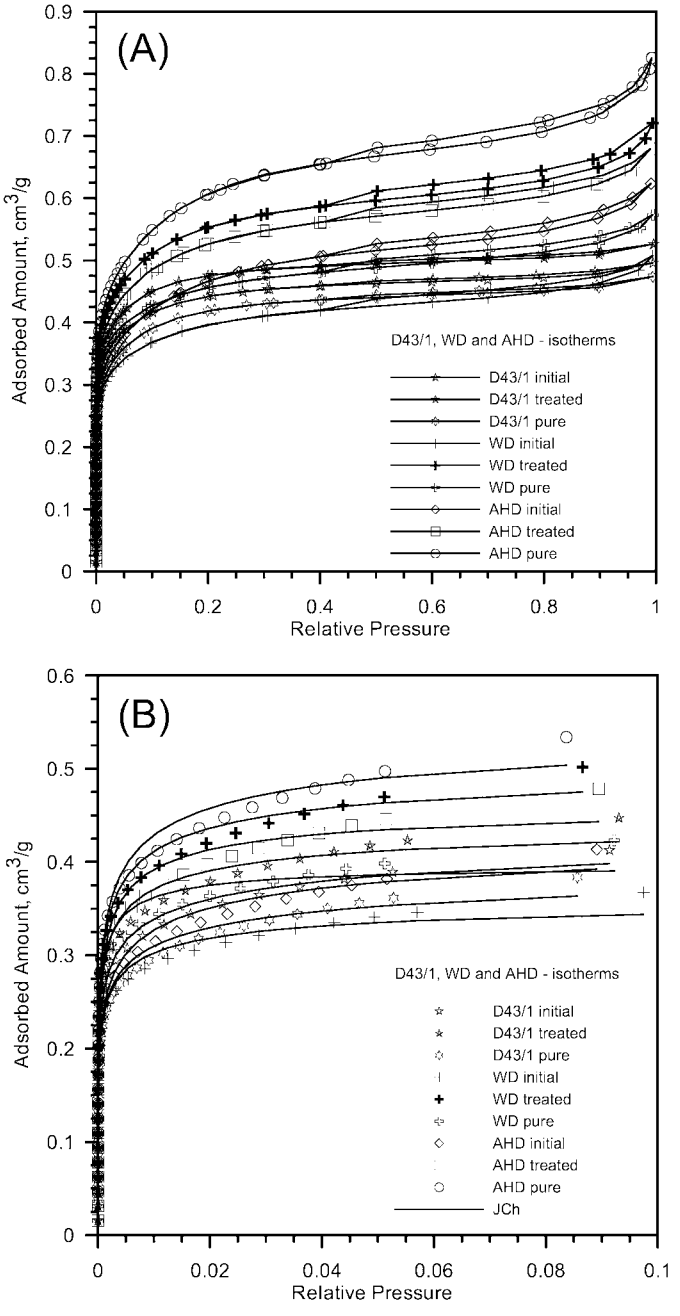

FIG. 8. (A) Low temperature (77.5 K) nitrogen adsorption—desorption isotherms for the AHD, D43/1 and WD activated carbons. (B) Results of fitting JCh equation (lines; Eq. [25]) to adsorption data (symbols).

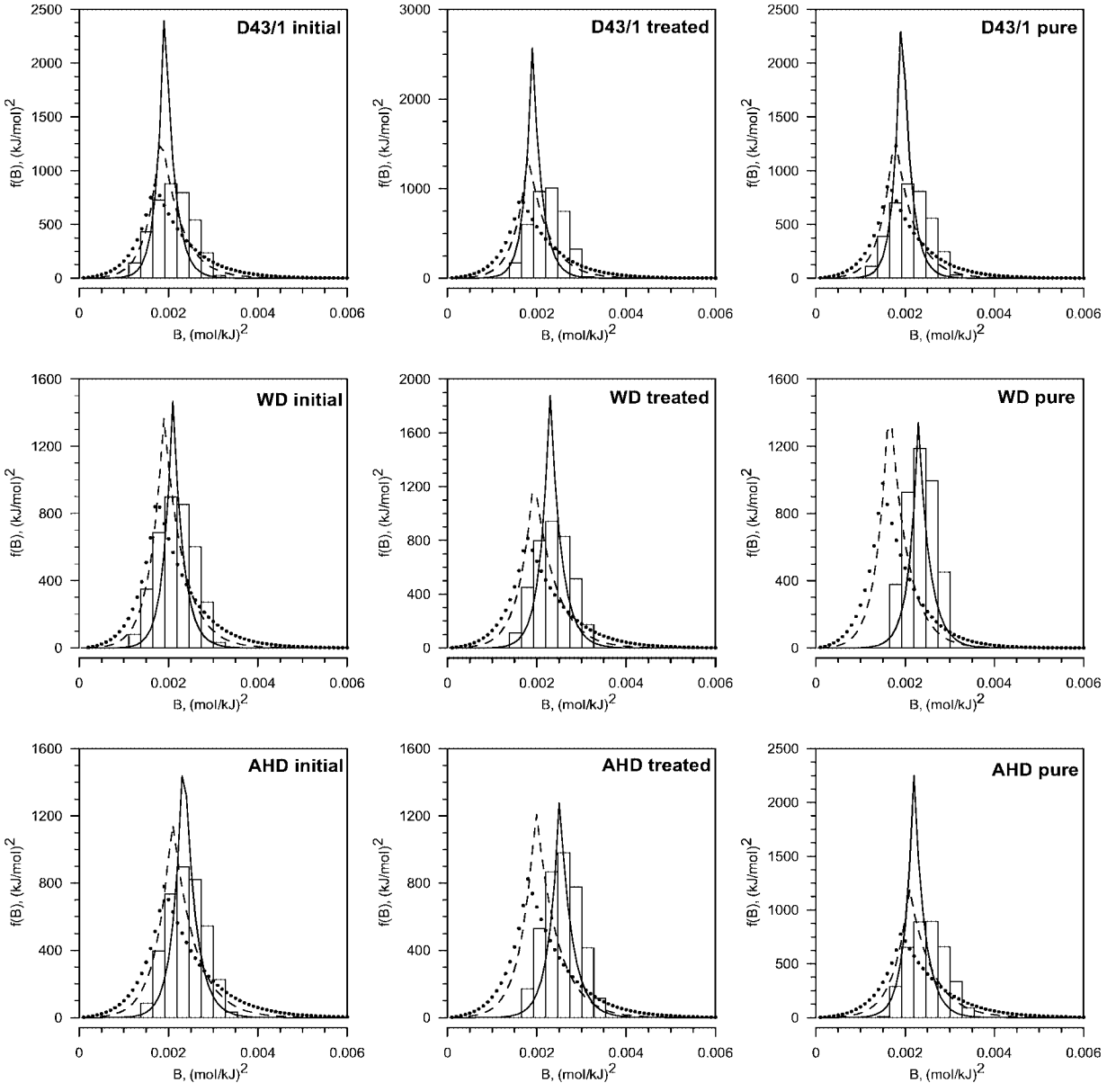

FIG. 9. Distributions of structural DR parameter $f(B)$ for selected unmodified and modified activated carbons (bar CONTIN algorithm, solid line (—) LAPLACE algorithm with $\omega = 10$, dashed line (---) LAPLACE algorithm with $\omega = 5$, and circles (• • •) LAPLACE algorithm with ($\omega = 3$)).

ones as well as than those obtained by means of the CONTIN algorithm. In the case of isotherms disturbed with Gaussian errors, the CONTIN algorithm reproduces the PSD peaks characterized by similar positions but greater variances than true MPSD (Fig. 7); however, the difference found can be reduced by additional variation of the regularization parameter in CONTIN. On the other hand, the LAPLACE algorithm preserves both positions and variances of generated peaks. In this case, the algorithm generates narrower and higher curves than true MPSD, but the obtained solutions seem to be very stable and free from Gaussian errors.

Second, the properties of the samples of microporous activated carbons (initial, treated, and pure) are investigated by all methods and algorithms mentioned above. Experimental nitrogen adsorption isotherms measured at 77.5 K are shown in Fig. 8A. It should be noted that all isotherms possess very similar shapes and are characterized by a narrow adsorption hysteresis loop (i.e., the mesoporosity and external surface are small) (79). Chemical processes such as treatment with concentrated HCl and HF influence only the adsorption capacity of modified samples of investigated adsorbents. Since the shape of nitrogen adsorption isotherms for unmodified and modified samples are very similar, one can expect that these processes mainly influence the chemical surface topography and do not influence the structure of pores (79). Comparison of the distributions of the structural parameter $f(B)$ and the MPSDs obtained by means

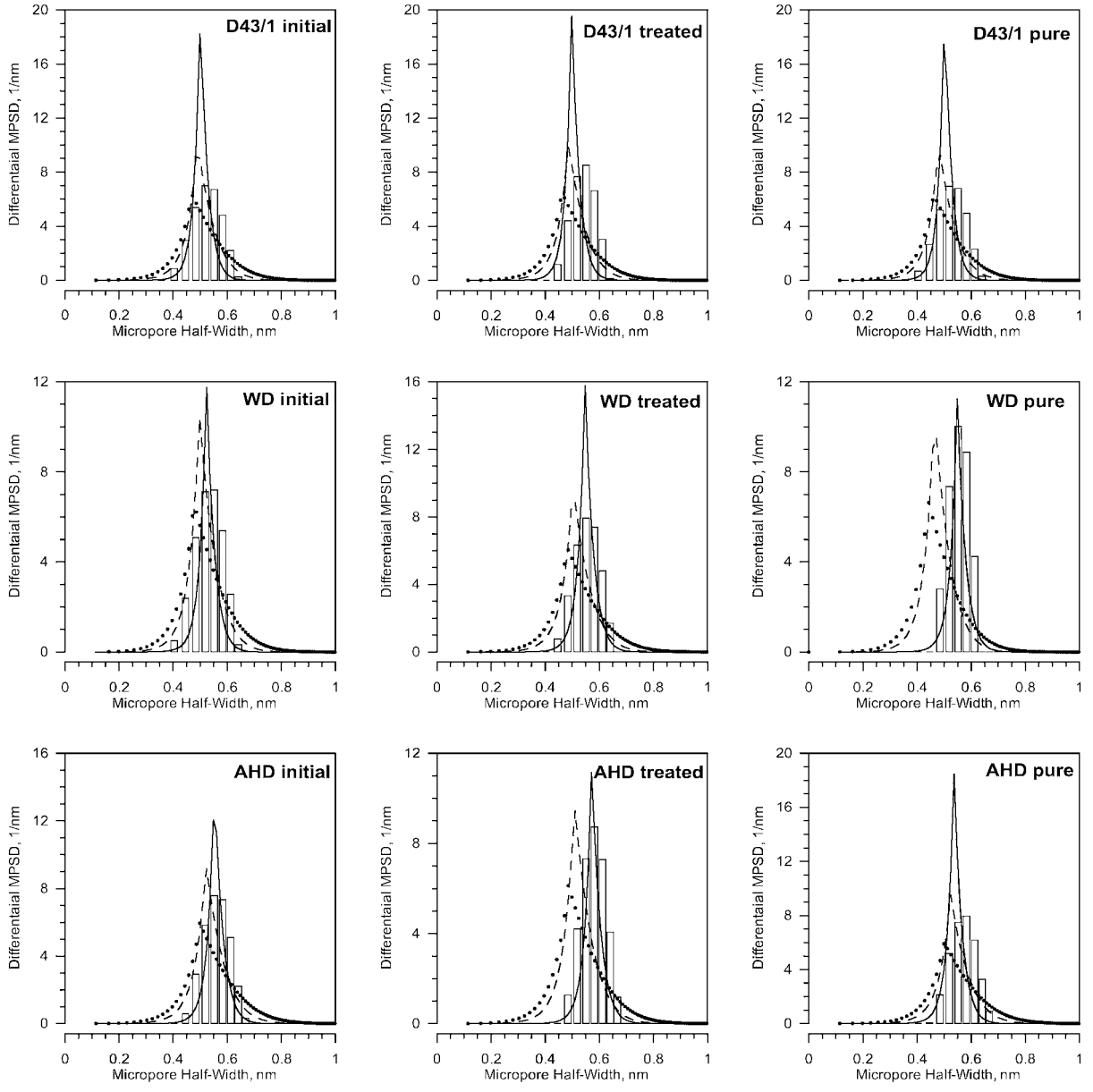

FIG. 10. Distributions of pore half-width for selected unmodified and modified activated carbons (bar CONTIN algorithm, solid line (—) LAPLACE algorithm with $\omega = 10$, dashed line (---) LAPLACE algorithm with $\omega = 5$, and circles (• • •) LAPLACE algorithm with ($\omega = 3$)).

of the CONTIN and LAPLACE algorithms for all investigated samples of activated carbons are presented in Figs. 9 and 10, respectively. Both algorithms generate monomodal $f(B)$ and MPSD. At first sight, all samples are characterized by very similar microporosity, and the pores are grouped generally in the range from 0.4 to 0.65 nm (for micropore half-width). For each sample, the LAPLACE algorithm reduces the assumed biporous structure of micropores to one peak. The parameter ω, influencing mainly the dispersion of base functions (see Eq. [18]), does not drastically affect received results (see Figs. 9 and 10). Note that the best correlation between the LAPLACE and CONTIN algorithms was obtained at $\omega = 10$. Final results are summarized in Table 1.

The results obtained using the DFT and ND methods are similar (see Figs. 11 and 12 and Table 2). Both methods suggest a bimodal structure of pores and indicate that chemical treatment does not significantly influence the pore structure of tested samples. But one should notice that the method proposed by Nguyen and Do slightly shifts the average dimension of pores to higher diameters (see Table 2) (35).

Another important conclusion is that HK results approximate DFT ones reasonably well (see Table 2 and Figs. 11 and 13). This method generates exponentially decreasing curves for all the examined samples of activated carbons, and like other methods it shows little difference in the pore structure of all investigated carbons.

TABLE 1

Structural Parameters Describing PSDs and MPSDs for All Investigated Samples of Activated Carbons: LAPLACE—New Algorithm Projected for Solution of Integral Adsorption Equation with DR or DA Equation as a Kernel, CONTIN—Provencher's Algorithms Modified to the Solution of Integral Adsorption Equations with DR Equation as a Kernel

Method	ω	Pore half-width range Δ nm	Para.	WD			AHD			D43/1		
				initial	treated	pure	initial	treated	pure	initial	treated	pure
LAPLACE	3	$\Delta < 1.0$	Ω	1.00	1.00	1.00	1.00	0.98	0.99	1.01	1.01	0.98
			$\bar{\varsigma}$, nm	0.51	0.52	0.48	0.54	0.53	0.54	0.51	0.50	0.50
			δ	8.0e-3	9.1e-3	7.6e-3	9.8e-3	9.1e-3	9.7e-3	8.6e-3	8.4e-3	8.4e-3
			σ	0.09	0.10	0.09	0.09	0.09	0.10	0.09	0.09	0.09
			χ	3.1e-4	3.3e-4	2.6e-4	3.7e-4	3.1e-4	3.4e-4	3.1e-4	3.0e-4	2.9e-4
	5	$\Delta < 1.0$	Ω	1.00	1.00	0.99	0.98	0.98	1.00	1.00	1.01	0.97
			$\bar{\varsigma}$, nm	0.51	0.52	0.48	0.54	0.53	0.54	0.50	0.50	0.49
			δ	3.8e-3	4.4e-3	3.7e-3	4.5e-3	4.3e-3	4.7e-3	4.1e-3	4.0e-3	3.9e-3
			σ	0.06	0.06	0.06	0.07	0.07	0.07	0.06	0.06	0.06
			χ	4.2e-5	3.6e-5	2.9e-5	4.6e-5	3.9e-5	4.1e-5	3.4e-5	3.4e-5	3.1e-5
	10	$\Delta < 1.0$	Ω	0.64	0.89	0.63	0.79	0.66	1.01	1.00	1.02	0.97
			$\bar{\varsigma}$, nm	0.53	0.55	0.55	0.56	0.58	0.54	0.50	0.50	0.51
			δ	1.3e-3	1.4e-3	1.4e-3	1.5e-3	1.6e-3	1.4e-3	1.2e-3	1.2e-3	1.1e-3
			σ	0.04	0.04	0.04	0.04	0.04	0.04	0.03	0.03	0.03
			χ	−2.7e-6	−3.0e-6	−2.9e-6	−1.0e-7	−5.2e-7	−2.7e-6	−2.2e-6	−2.1e-6	−8.3e-7
CONTIN		$0.4 < \Delta < 0.7$	Ω	1.02	1.03	1.06	1.01	1.04	1.03	1.02	1.03	1.00
			$\bar{\varsigma}$, nm	0.53	0.55	0.55	0.56	0.58	0.57	0.52	0.54	0.53
			δ	2.6e-3	2.2e-3	1.4e-3	2.3e-3	1.9e-3	2.1e-3	2.8e-3	1.9e-3	2.7e-3
			σ	0.05	0.05	0.04	0.05	0.04	0.05	0.05	0.04	0.05
			χ	−2.9e-5	−1.7e-5	−7.8e-6	−1.3e-5	−1.0e-5	−4.7e-6	−2.9e-5	−1.4e-5	−2.8e-5

TABLE 2

Structural Parameters Describing PSDs and MPSDs for All Investigated Samples of Activated Carbons: DFT—Density Functional Theory, ND—Nguyen and Do Method, HK—Horvath and Kawazoe Equation

Method	Pore half-width range Δ nm	Para.	WD			AHD			D43/1		
			initial	treated	pure	initial	treated	pure	initial	treated	pure
DFT	$\Delta < 0.5$	Ω	0.41	0.13	0.44	0.09	0.20	0.12	0.44	0.45	0.35
		$\bar{\varsigma}$, nm	0.37	0.42	0.38	0.40	0.39	0.40	0.37	0.33	0.36
		δ	6.7e-4	1.8e-4	5.8e-4	5.1e-4	5.0e-4	5.1e-4	6.6e-4	3.2e-3	3.8e-4
		σ	0.03	0.01	0.02	0.02	0.02	0.02	0.03	0.06	0.02
		χ	1.5e-5	−3.6e-7	3.7e-6	−1.8e-6	7.5e-8	−2.1e-6	1.5e-5	9.2e-5	4.0e-6
	$0.5 < \Delta < 2$	Ω	0.45	0.62	0.41	0.54	0.50	0.56	0.50	0.48	0.56
		$\bar{\varsigma}$, nm	0.87	0.87	0.87	0.93	0.87	0.90	0.81	0.78	0.85
		δ	9.6e-2	8.5e-2	9.5e-2	1.0e-1	9.1e-2	9.4e-2	6.6e-2	5.0e-2	6.3e-2
		σ	0.31	0.29	0.31	0.32	0.30	0.31	0.26	0.22	0.25
		χ	0.03	0.03	0.03	0.03	0.03	0.02	0.02	0.01	0.02
ND	$\Delta < 0.7$	Ω	0.25	0.31	0.31	0.29	0.31	0.31	0.29	0.26	0.25
		$\bar{\varsigma}$, nm	0.47	0.47	0.47	0.48	0.47	0.47	0.46	0.47	0.46
		δ	5.5e-4	2.5e-4	2.5e-4	2.5e-3	2.6e-4	4.7e-4	6.4e-4	2.9e-4	3.9e-3
		σ	0.02	0.02	0.02	0.05	0.02	0.02	0.03	0.02	0.02
		χ	1.4e-5	1.1e-6	1.1e-6	3.1e-4	8.6e-9	9.4e-6	1.0e-5	4.8e-6	1.1e-5
	$0.5 < \Delta < 2.5$	Ω	0.17	0.26	0.26	0.22	0.25	0.30	0.18	0.18	0.19
		$\bar{\varsigma}$, nm	1.10	1.08	1.08	1.16	1.11	1.08	0.96	0.97	0.95
		δ	0.16	0.15	0.15	0.12	0.15	0.13	0.10	0.14	0.10
		σ	0.40	0.39	0.39	0.35	0.39	0.36	0.32	0.38	0.32
		χ	0.05	0.06	0.06	0.04	0.05	0.04	0.05	0.10	0.05
HK	$0.2 < \Delta < 0.9$	Ω	0.90	0.91	1.02	0.89	0.99	0.89	0.82	0.97	0.93
		$\bar{\varsigma}$, nm	0.38	0.40	0.36	0.40	0.38	0.41	0.40	0.37	0.39
		δ	2.3e-2	2.5e-2	2.2e-2	2.6e-2	2.4e-2	2.6e-2	2.3e-2	2.3e-2	2.5e-2
		σ	0.15	0.16	0.15	0.16	0.16	0.16	0.15	0.15	0.16
		χ	4.4e-3	4.1e-3	4.7e-3	4.3e-3	2.5e-3	4.2e-3	3.9e-3	4.4e-3	4.3e-3

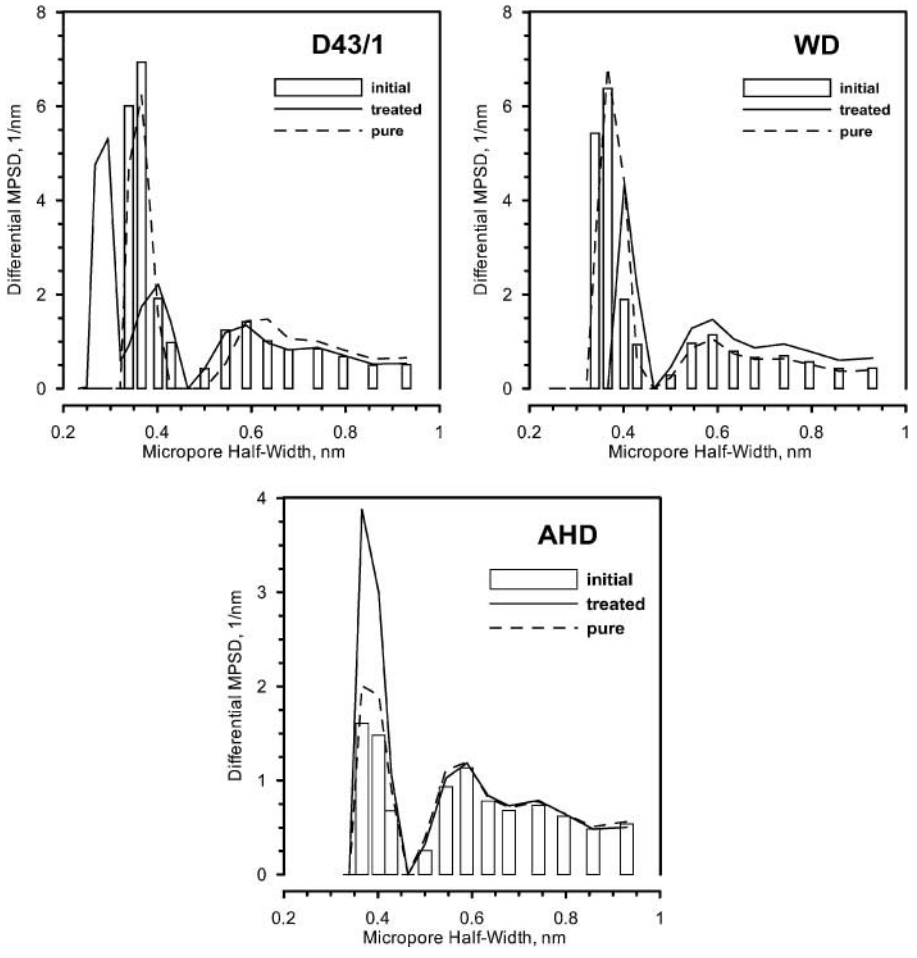

FIG. 11. DFT pore size distributions for selected unmodified and modified activated carbons (only the range of micropores is shown).

The comparison of experimental and theoretical (i.e., obtained by fitting of the JCh equation to experimental data) nitrogen adsorption isotherms in the micropore region is depicted in Fig. 8B. For the fitting of the JCh equation to the measured data, the novel hybrid algorithm (i.e., consisting of the evolutionary algorithm (EVOL) (60) and the simplex method proposed by Nelder and Mead) (78) was applied. In contrast to classical optimization methods such algorithms are resistant to local extremes. The obtained results show that despite good fitting of theoretical data to experimental ones the obtained parameters of the JCh equation both do not possess physical meaning and do not generate the MPSD (see Table 3).

The APDs for the all examined carbons are presented in Fig. 14. All curves possess very similar shapes. They are characterized by at least two distinct peaks observed around 8 kJ/mol and 2 kJ/mol. It is known that the first peak is responsible for one stage micropore filling lower than monolayer, and the second is related to the secondary micropore filling. For all samples, excluding WD carbons, an additional peak responsible for formation of the monolayer in micropores is visibly located close

TABLE 3
Parameters of JCh Equation Obtained for All Tested Samples of Activated Carbons

	WD			AHD			D43/1		
Parameter	initial	treated	pure	initial	treated	pure	initial	treated	pure
W_0 cm^3/g	0.36	0.50	0.39	0.42	0.46	0.53	0.42	0.44	0.39
ρ	2.3e10	1.6e10	3.5e11	9.9e9	6.7e10	1.7e10	5.3e9	3.8e10	1.0e10
ν	1.6e7	1.5e7	1.9e7	2.6e7	2.2e7	2.3e7	1.3e7	2.5e7	2.4e7
n	2.35	2.29	3.18	1.97	2.64	2.19	1.95	2.38	1.96
SSD	3.3e-3	1.0e-2	1.7e-2	4.3e-3	1.6e-2	9.6e-3	2.6e-3	7.5e-3	1.2e-2

TABLE 4

Energetic Parameters Describing AEDs for All Investigated Samples of Activated Carbons: FG—Solution of Adsorption Integral Equation with Fowler–Guggenheim Equation as a Kernel

Method	Adsorption energy range Δ kJ/mol	Para.	WD			AHD			D43/1		
			initial	treated	pure	initial	treated	pure	initial	treated	pure
FG	$\Delta < 8$	Ω	0.39	0.39	0.30	0.44	0.37	0.44	0.11	0.41	0.37
		$\bar{\varepsilon}$, kJ/mol	5.06	4.91	4.74	5.09	4.80	5.11	3.97	5.17	5.01
		δ	0.85	0.70	0.54	0.89	0.59	0.88	0.09	0.92	0.73
		σ	0.92	0.84	0.74	0.94	0.77	0.94	0.30	0.96	0.86
		χ	0.21	0.15	0.06	0.24	0.09	0.23	−0.01	0.23	0.05
	$8 < \Delta < 12$	Ω	0.31	0.31	0.28	0.35	0.31	0.35	0.24	0.37	0.24
		$\bar{\varepsilon}$, kJ/mol	8.99	8.53	7.77	9.26	8.09	9.14	8.55	9.37	7.95
		δ	1.01	0.88	0.64	1.19	0.74	1.05	0.64	1.00	0.68
		σ	1.00	0.94	0.80	1.09	0.86	1.02	0.80	1.00	0.82
		χ	−0.07	0.01	0.03	−0.12	0.05	−0.07	−0.07	−0.03	0.18
	$12 < \Delta < 16$	Ω	0.48	0.53	0.62	0.39	0.54	0.41	0.50	0.43	0.58
		$\bar{\varepsilon}$, kJ/mol	12.78	12.30	12.06	12.92	12.15	12.74	12.87	13.17	12.53
		δ	0.91	0.83	0.47	0.96	0.51	0.84	1.67	0.68	1.48
		σ	0.95	0.91	0.68	0.98	0.72	0.92	1.29	0.83	1.22
		χ	−0.04	−0.04	−0.03	0.15	−0.04	0.05	0.60	−0.10	−0.33

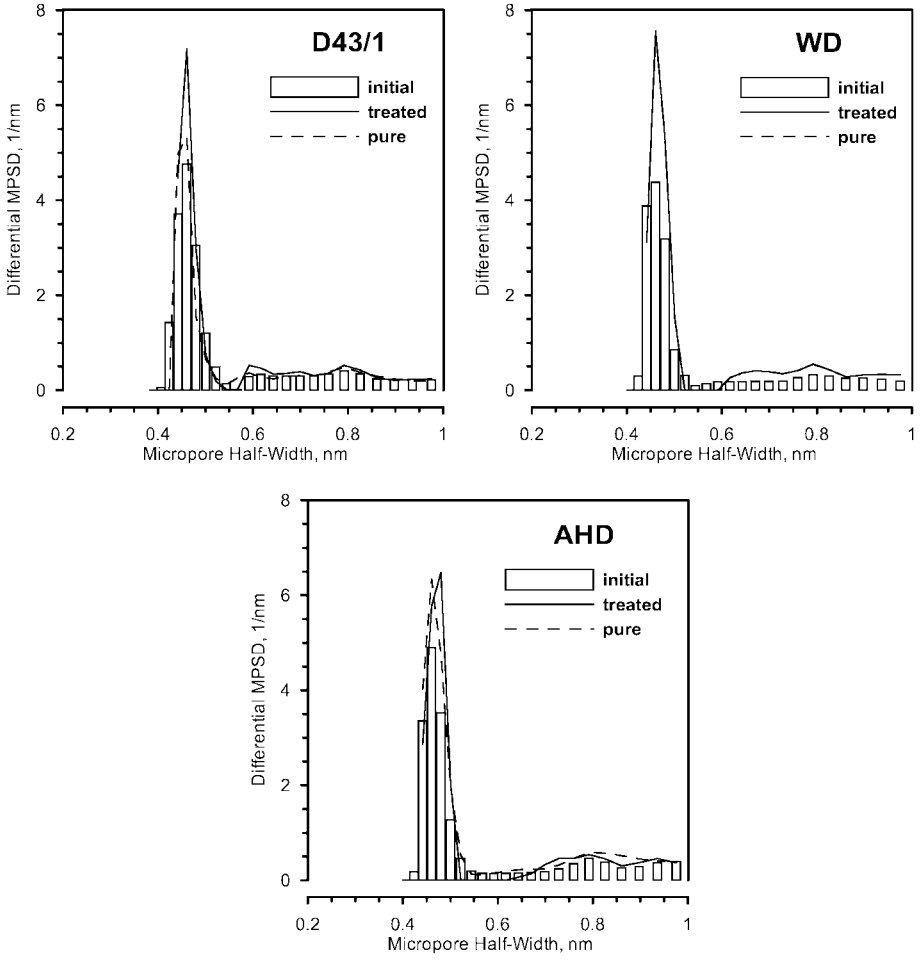

FIG. 12. Pore size distributions for selected unmodified and modified activated carbons obtained on the basis Nguyen and Do method (only the range of micropores is shown).

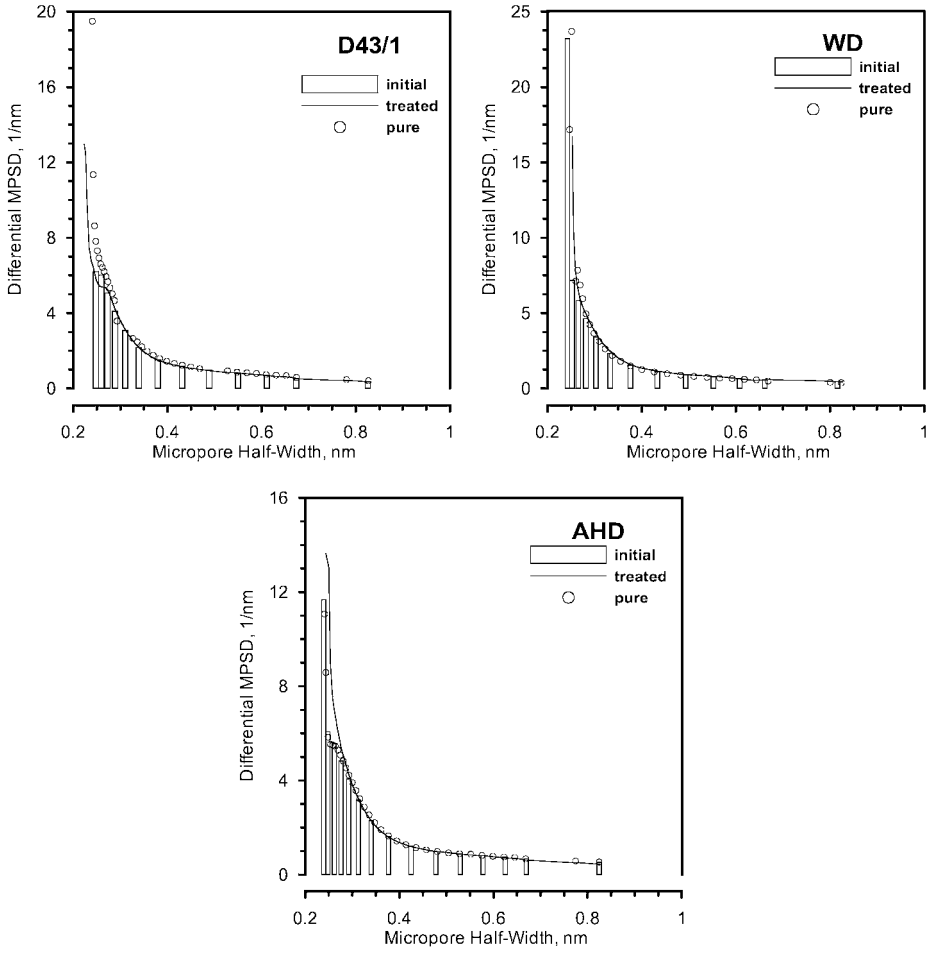

FIG. 13. HK MPSDs for selected unmodified and modified activated carbons.

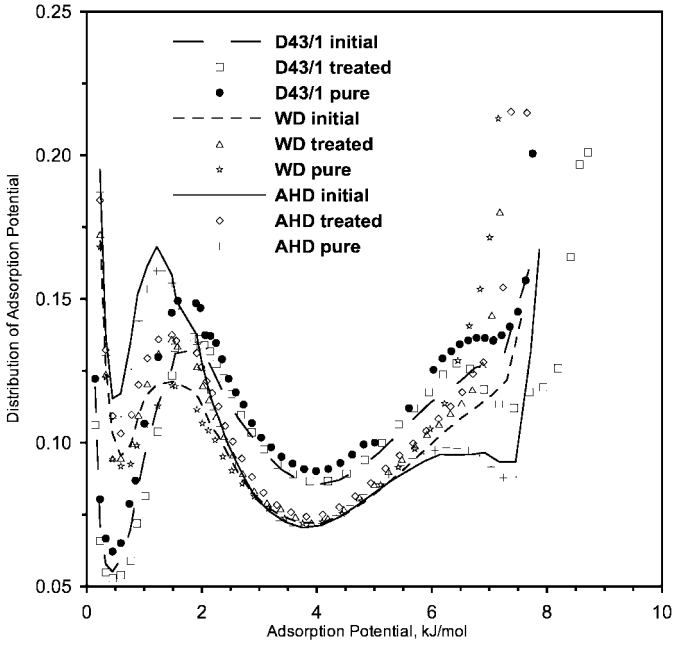

FIG. 14. APDs for selected unmodified and modified activated carbons.

to 6 kJ/mole. Thus, the shapes of the obtained distributions suggest, as pointed out by Gun'ko and Do (35), that each of the investigated samples of activated carbons is microporous and is characterized by a small quantity of mesopores.

The AEDs obtained using the Fowler–Guggenheim equation as a kernel of the integral Fredholm equation with respect to the adsorption energy for all the investigated carbons are compared in Fig. 15. First of all, this method is more practical than APDs. The peaks are strongly marked, and what is also important, the limits of the energy are finite (at $p/p_0 \to 0$ and/or $p/p_0 \to 1$). Both the adsorption energy range and the shape (three modals) of AEDs for tested samples of activated carbons are very similar. Comparing the obtained PSDs as well as APD and AED curves, one can conclude that obtained materials are structurally as well as energetically heterogeneous. Comparing energy distributions (Figs. 14 and 15 and Table 4) it can be seen that despite the shift of both distributions along the energy axis (caused by the entropy term) the peaks on AEDs are clearly visible and can be easier distinguished than on APD curves. What is more important, the peak close to 6 kJ/mol for WD carbon is practically invisible on APD curves, and is still present on AE distributions. Thus, despite the simplicity of calculation of APDs, the AED curves are

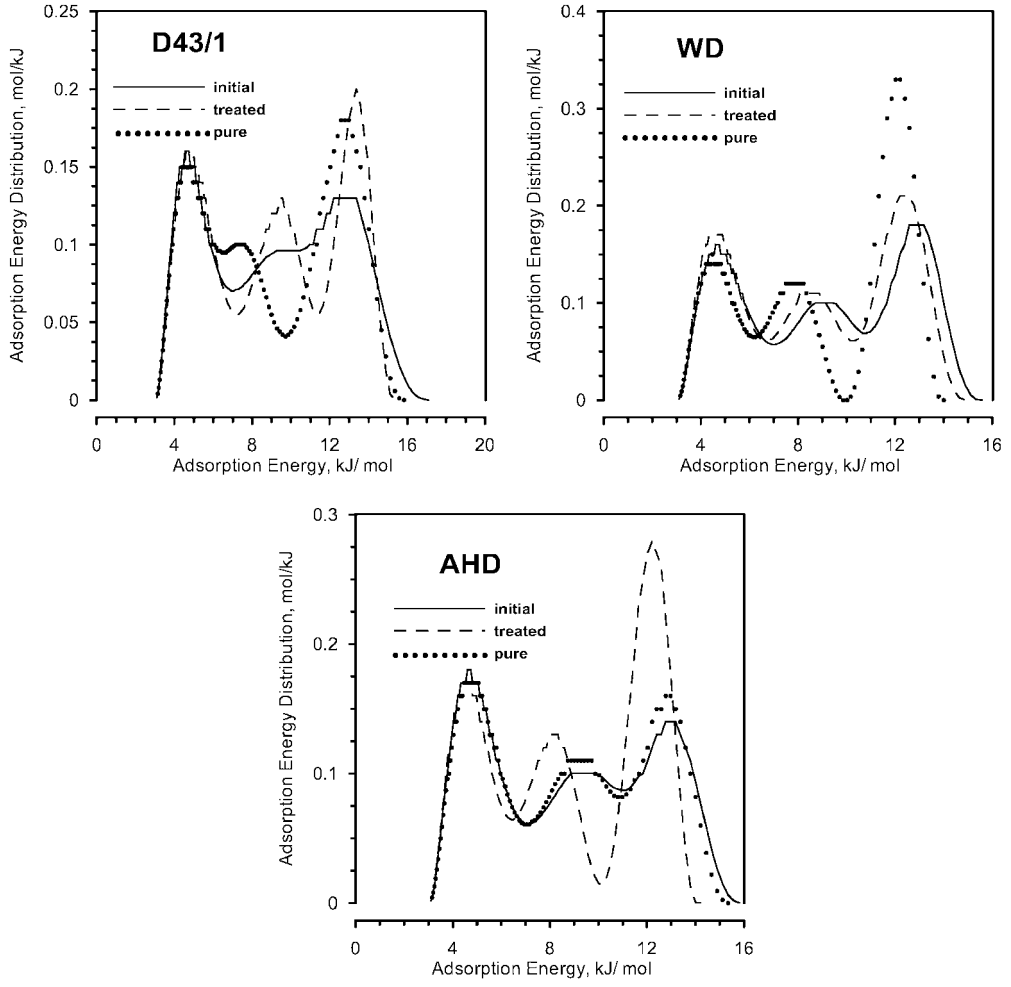

FIG. 15. Adsorption energy distributions for selected unmodified and modified activated carbons computed with (Eqs. [35 and 36]).

more sensitive to the changes in the structure of adsorbents. The interpretation of the position of energy peaks obtained from the method studied was recently studied by Puziy and co-workers (46). It was established that the peak in the range of 8 kJ/mol is attributed to interaction between the nitrogen molecules and the basal planes of graphitic microcrystallites (i.e., the formation of monolayer on the walls of wider micropores). The peak at 5 kJ/mol is attributed to secondary micropore filling on polymolecular adsorption (nitrogen liquefaction heat 5.6 kJ/mol). One can, however, pay back attention to the intensity of each peak. And thus, during the chemical modification of initial samples of activated carbons, the intensity of the high-energy peak, attributed to the presence of micropores ($E \approx \langle 12, 13 \rangle$ kJ/mol), changes significantly (Table 4).

CONCLUSIONS

The presented study deals with the methods of characterization of structural and energetic heterogeneity of microporous carbons. Different methods are compared and a new one called LAPLACE is proposed. The SGA algorithm is modified and applied for this purpose. The power of the CONTIN and LAPLACE algorithms was checked. It is shown that both methods recover mono- and bimodal $f(B)$, as well as MPSD curves, reasonably well. The main advantage of LAPLACE is that the obtained solutions seem to be very stable and free from Gaussian errors. Moreover, the LAPLACE procedure is simpler and quicker than CONTIN. The fit of the experimental data by the LAPLACE algorithm leads to a very good correlation between this method and CONTIN, and the best fit is obtained for the parameter $\omega = 10$. Therefore LAPLACE can be successfully applied to the characterization of microporous solids.

The method proposed by Nguyen and Do leads to almost the same results as obtained from DFT theory; however, the ND method slightly shifts the average dimension of pores to higher diameters. The HK method leads to average pore diameters similar to those found by the DFT method. The process of deashing of carbons changes the energetic heterogeneity of studied carbons, what is clearly visible on the APD as well as AED curves. The AED seems to lead to more realistic results than APD does;

however, to check the reality of the results of both methods the comparison with calorimetric measurements of the enthalpy of adsorption is necessary to be carried out. This problem will be studied in the near future.

REFERENCES

1. Rudziński, W., and Everett, D. H., "Adsorption of Gases on Heterogeneous Surfaces." Academic Press, New York, 1992.
2. Rudziński, W., Steele, W. A., and Zgrablich, G., Eds. "Equilibria and Dynamics of Gas Adsorption on Heterogeneous Solid Surfaces." Elsevier, Amsterdam, 1997.
3. Wojsz, R., "Characteristics of the Structural and Energetic Heterogeneity of Microporous Carbon Adsorbents Regarding the Adsorption of Polar Substances." UMK, Toruń, 1989. [In Polish]
4. Do, D. D., "Adsorption Analysis: Equilibria and Kinetics." Imperial College Press, London, 1998.
5. Jankowska, H., Świątkowski, A., and Choma, J., "Węgiel aktywny." WNT, Warsaw, 1985.
6. Everett, D. H., *Trans. Faraday Soc.* **46,** 46 (1990).
7. Dubinin, M. M., "Adsorption and Porosity." WAT, Warsaw, 1975. [In Polish]
8. Gregg, S. J., and Sing, K. S. W., "Adsorption, Surface Area and Porosity." Academic Press, London, 1982.
9. Cerofolini, G. F., and Re, N., *Riv. Nuovo Cimento* **16,** 1 (1993).
10. Gauden, P. A., "Theoretical Description of the Structural and Energetic Heterogeneity of Carbonaceous Materials" (Thesis). UMK, Toruń, 2001. [In Polish]
11. Jagiełło, J., and Schwarz, J. A., *Langmuir* **9,** 2513 (1993).
12. Press, W. H., Teukolsky, S. A., Vetterling, W. T., and Flannery, B. P., "Numerical Recipes in Fortran." Cambridge Univ. Press, Cambridge, UK, 1992.
13. Tikhonov, A. N., *Dokl. Akad. Nauk USSR* **39,** 195 (1943).
14. Phillips, D. L., *J. Assoc. Comput. Mach.* **9,** 84 (1962).
15. Morozov, V. A., "Methods for Solving Incorrectly Posed Problems." Springer-Verlag, Berlin, 1984.
16. Olivier, J. P., and Conklin, W. B., "Proceedings of the First International Symposium on Effect of Surface Heterogeneity in Adsorption and Catalysis on Solids." Kazimierz Dolny, 1992.
17. Szombathely, M., v., Brauer, M., and Jaroniec, M., *J. Comput. Chem.* **13,** 17 (1992).
18. Bhatia, S. K., and Chakraborty, D., *AIChE J.* **38,** 868 (1992).
19. Michalewicz, Z., "Genetic Algorithms + Data Structures = Evolutions Programs." Springer-Verlag, Berlin, 1996.
20. Provencher, S. W., *Comput. Phys. Commun.* **27,** 213 (1982).
21. Provencher, S. W., *Comput. Phys. Commun.* **27,** 229 (1982).
22. Toth, J., *Adv. Colloid Interface Sci.* **55,** 54 (1995).
23. Toth, J., *J. Colloid Interface Sci.* **163,** 299 (1994).
24. Condon, J. B., *Micropor. Mesopor. Mater.* **38,** 359 (2000).
25. Condon, J. B., *Micropor. Mesopor. Mater.* **38,** 377 (2000).
26. Jaroniec, M., Lu, X., and Madey, R., *Monatsh. Chem.* **122,** 577 (1991).
27. Oliver, J. P., *J. Porous Mater.* **2,** 9 (1995).
28. Seaton, N. A., Walton, J. P. R. B., and Quirke, N. A., *Carbon* **27,** 853 (1989).
29. Olivier, J. P., Conklin, W. B., v., and Szombathley, M., *Stud. Surf. Sci. Catal.* **87,** 81 (1994).
30. Gac, W., Patrykiejew, A., and Sokołowski, S., *Thin Solid Films* **22,** 298 (1997).
31. Lastoskie, C. M., Gubbins, K. E., and Quirke, N., *Langmuir* **9,** 2693 (1993).
32. Nguyen, C., and Do, D. D., *Langmuir* **15,** 3608 (1999).
33. Nguyen, C., and Do, D. D., *Langmuir* **16,** 7218 (2000).
34. Nguyen, C. D., and Do, D. D., *Colloids Surf. A* **187,** 51 (2001).
35. Gun'ko, V. M., and Do, D. D., *Colloids Surf. A* **193,** 71 (2001).
36. Horvath, G., and Kawazoe, K., *J. Chem. Engn. Jpn.* **16,** 6 (1983).
37. Horvath, G., *Colloids Surf. A* **141,** 295 (1998).
38. Terzyk, A. P., Gauden, P. A., Rychlicki, G., and Wojsz, R., *Carbon* **36,** 1703 (1998).
39. Terzyk, A. P., Gauden, P. A., Rychlicki, G., and Wojsz, R., *Carbon* **37,** 539 (1999).
40. Gauden, P. A., and Terzyk, A. P., *J. Colloid Interface Sci.* **227,** 482 (2000).
41. Kowalczyk, P., Terzyk, A. P., Gauden, P. A., and Solarz, L., *Computers Chem.* **26,** 125 (2002).
42. Świątkowski, A., Trznadel, B. J., and Zięteк, S., *Adsorpt. Sci. Technol.* **14,** 59 (1996).
43. Kruk, M., Jaroniec, M., and Gadkaree, K. P., *Langmuir* **15,** 1442 (1999).
44. Choma, J., and Jaroniec, M., *Langmuir* **13,** 1026 (1997).
45. Mamleev, V. Sh., and Bekturov, E. A., *Langmuir* **12,** 3630 (1996).
46. Puziy, A. M., Matynia, T., Gawdzik, B., and Poddubnaya, O. I., *Langmuir* **15,** 6016 (1999).
47. Dubinin, M. M., and Stoeckli, F., *J. Colloid Interface Sci.* **75,** 34 (1980).
48. Terzyk, A. P., and Gauden, P. A., *Colloids Surf. A* **57,** 177 (2001).
49. Bhatia, S. K., and Shethna, H. K., *Langmuir* **10,** 3230 (1994).
50. Terzyk, A. P., Gauden, P. A., Zawadzki, J., Rychlicki, G., Winiewski, M., and Kowalczyk, P., *J. Colloid Interface Sci.* **243,** 183 (2001).
51. Dubinin, M. M., Plavnik, G. N., and Zaverina, E. D., *Carbon* **2,** 261 (1964).
52. Gun'ko, V. M., Leboda, R., Skubiszewska-Zięba, J., Turov, V. V., and Kowalczyk, P., *Langmuir* **17,** 3148 (2001).
53. Gun'ko, V. M., Leboda, R., Marciniak, M., Grzegorczyk, W., Skubiszewska-Zieba, J., Malygin, A. A., and Malkov, A. A., *Langmuir* **16,** 3227 (2000).
54. Puziy, A. M., Poddubnaya, O. I., Ritter, J. A., Ebner, A. D., and Holland, Ch. E., *Carbon* **39,** 2313 (2001).
55. Leboda, R., Gun'ko, V. M., Tomaszewski, W., and Trznadel, B. J., *J. Colloid Interface Sci.* **238,** 489 (2001).
56. Leboda, R., Turov, V. V., Tomaszewski, W., Skubiszewska-Zięba, J., and Gun'ko, V. M., *Carbon*, in press (2002).
57. Leboda, R., Turov, V. V., Tomaszewski, W., Gun'ko, V. M., and Skubiszewska-Zięba, J., *J. Colloid Interface Sci.*, in press.
58. Gun'ko, V. M., Leboda, R., Turov, V. V., Villiéras, F., Skubiszewska-Zięba, J., Chodorowski, S., and Marciniak, M., *J. Colloid Interface Sci.* **238,** 340.
59. Kowalczyk, P., Terzyk, A. P., and Gauden, P. A., *Langmuir* (in press).
60. Kowalczyk, P., Szmigielski, R., Terzyk, A. P., Gauden, P. A., Zięteк, S., and Palijczuk, D., *Bull. WIChiR*, in press. [In Polish]
61. Provencher, S. W., "CONTIN Users Manual," Version 2. Max-Planck-Institut für Biophysikalische Chemie, Göttingen, 1984.
62. Holland, J. H., "Adaptation in Natural and Artificial Systems." Univ. of Michigan Press, Ann Arbor, 1975.
63. Goldberg, D. E., "Genetic Algorithms in Search, Optimisation and Machine Learning." Addison–Wesley, Reading, MA, 1989.
64. Terzyk, A. P., Wojsz, R., Rychlicki, G., and Gauden, P. A., *Colloids Surf. A* **119,** 175 (1996).
65. Terzyk, A. P., Wojsz, R., Rychlicki, G., and Gauden, P. A., *Colloids Surf. A* **126,** 67 (1997).
66. Terzyk, A. P., Wojsz, R., Rychlicki, G., and Gauden, P. A., *Colloids Surf. A* **136,** 245 (1998).
67. Terzyk, A. P., Gauden, P. A., Rychlicki, G., and Wojsz, R., *Colloids Surf. A* **152,** 293 (1999).
68. Terzyk, A. P., Gauden, P. A., Rychlicki, G., and Wojsz, R., *Langmuir* **15,** 285 (1999).
69. Gauden, P. A., Terzyk, A. P., and Rychlicki, G., *Carbon* **39,** 267 (2001).
70. Kowalczyk, P., Terzyk, A. P., and Gauden, P. A., *J. Colloid Interface Sci.* **243,** 300 (2001).
71. Yin, Y. F., McEnaney, B., and Mays, T. J., *Carbon* **36,** 1452 (1998).
72. Nicholson, D., *Langmuir* **15,** 2508 (1999).
73. Henderson, D., Patrykiejew, A., Pizio, O., and Sokołowski, S., *Physica A* **233,** 67 (1996).
74. Webb, P. A., and Orr, C., "Analytical Methods in Fine Particle Technology." Micrometrics Instrument Corp., Norcross, GA, 1997.
75. Gauden, P. A., and Terzyk, A. P.,"Theory of Adsorption in Micropores of Carbonaceous Materials." Wichir, Warsaw, 2002. [In Polish]

76. Cooper, B. E., "Statistics for Experimentalists." Pergamon, Oxford, 1969.
77. Back, T., Fogel, D., and Michalewicz, Z., Eds. "Handbook of Evolutionary Computation." Oxford Univ. Press, New York, 1996.
78. Schwefel, H. P., "Evolution and Optimum Seeking." Wiley, Chichester, 1995.
79. Rychlicki, G., Terzyk, A. P., and Majchrzycki, W., *J. Chem. Technol. Biotechnol.* **74,** 329 (1999).
80. Terzyk, A. P., *Adsorpt. Sci. Technol.* **17,** 441 (1999).
81. Terzyk, A. P., and Rychlicki, G., *Colloids Surf. A* **163,** 135 (2000).
82. Terzyk, A. P., *Adsorpt. Sci. Technol.* **18,** 477 (2000).
83. Terzyk, A. P., *J. Colloid Interface Sci.* **230,** 219 (2000).
84. Terzyk, A. P., *Colloids Surf. A* **177,** 23 (2001).
85. Terzyk, A. P., and Gauden, P. A., *Sep. Sci. Technol.* **36,** 513 (2001).
86. Terzyk, A. P., and Gauden, P. A., *J. Colloid Interface Sci.* **249,** 256 (2002).
87. Terzyk, A. P., *J. Colloid Interface Sci.* **247,** 507 (2002).